ELSEVIER

Journal of Hazardous Materials B80 (2000) 241–257

Journal of Hazardous Materials

www.elsevier.nl/locate/jhazmat

A kinetic model for the degradation of benzothiazole by Fe^{3+}-photo-assisted Fenton process in a completely mixed batch reactor

Roberto Andreozzi*, Antonio D'Apuzzo, Raffaele Marotta

Dipartimento di Ingegneria Chimica, Facoltà di Ingegneria, Università di Napoli "Federico II", p.le V. Tecchio, 80125 Napoli, Italy

Received 27 March 2000; received in revised form 9 August 2000; accepted 15 August 2000

Abstract

The degradation of benzothiazole in aqueous solution by a photo-assisted Fenton reaction has been studied in a batch reactor in the pH range 2.0–3.2 and for H_2O_2 and Fe(III) concentrations respectively between 1.0×10^{-3}–1.5×10^{-1} and 1.0×10^{-6}–4.0×10^{-6} M.

A kinetic model has been developed to predict the decay of benzothiazole at varying reaction conditions. The use of kinetic constants from the literature in the model allows to simulate the system behavior by taking into account the influence of pH, hydrogen peroxide, Fe(III) and sulfate concentrations and the ionic strength. © 2000 Elsevier Science B.V. All rights reserved.

Keywords: Benzothiazoles; Advanced oxidation process; Photo-Fenton system; Kinetic model; Hydrogen peroxide; Hydroxyl radical; Ferric ion; Wastewater treatment

1. Introduction

Among all the most well known system which allow the generation of OH radicals Fenton reaction is represented by the following reaction:

$$Fe^{II} + H_2O_2 \overset{k_{Fe^{II}/H_2O_2}}{\rightarrow} Fe^{III} + HO^- + HO^\bullet \quad (1)$$

In recent years, the possibility of utilizing the Fenton reaction for the oxidative treatment of wastewaters has been reported by several authors [1–3]. However, the limit of this system, that is, the need to use a stoichiometric amount of Fe(II) has turned attention to

* Corresponding author. Tel.: +39-81-7682251; fax: +39-81-5936936.
E-mail address: andreo@irc.na.cnr.it (R. Andreozzi).

0304-3894/00/$ – see front matter © 2000 Elsevier Science B.V. All rights reserved.
PII: S0304-3894(00)00308-3

mineral-catalyzed Fenton [4–6] or to a possible variation of reaction (1), the so-called photo-assisted Fenton system. The latter combines an ultraviolet light ($\lambda > 300$ nm), hydrogen peroxide and catalytic amounts of Fe(III) to produce HO radicals, according to the following reaction:

$$Fe(OH)^{2+} \xrightarrow{h\nu} HO^{\bullet} + Fe^{II} \quad (2)$$

as well as reaction (1). Although other reactions occur (see below), reactions (1) and (2) clearly elucidate the main feature of photo-assisted Fenton system, that is iron cycling between +2 and +3 oxidation states with HO production being only limited by H_2O_2 availability.

Following the papers of Pignatello and co-workers on the chlorophenoxy herbicides and dioxins [7,8], the degradation of a significant number of chemical pollutants by means of Fe^{3+}-photo-assisted Fenton has been studied [9–17], indicating much interest of researchers in this oxidative system. This interest is entirely explained if one considers that Fe^{3+}-photo-assisted Fenton along with titanium dioxide-mediated photocatalysis [18] are the oxidative systems which exploit solar energy for water and wastewater treatment.

In a previous paper [19], the oxidation of benzothiazole and two of its derivatives (MBT and OBT) was studied using of H_2O_2/UV and Fe^{3+}-photo-assited Fenton techniques.

The study of the oxidative treatments of these compounds has been undertaken due to their presence in industrial effluents and river waters [20–22] as well as doubt about their biodegradability [23–25]. In the same paper [19] a model which describes the benzothiazole derivatives behavior in H_2O_2/UV experiments has been developed too and used to obtain kinetic constants for HO radical attack to studied heterocyclics.

In the present paper the authors extend the kinetic modeling to simulate the decay of benzothiazole when it is subjected to an oxidative treatment by means of Fe^{3+}-photo-assisted Fenton and in which the role of buffering species (HSO_4^- and SO_4^{2-}) and ionic strength is accounted for.

2. Experimental

All the experiments were carried out at 293 K in an annular glass reactor equipped with a high pressure Hg lamp (UV 12F Helios Italquartz) of a nominal power of 125 W, mainly emitting at 305, 313 and 366 nm (manufacturer's data). The irradiated volume of the reactor (V_o) and the path length (L) were 0.28 l and 1.1 cm, respectively.

BT (benzothiazole), ferric perchlorate ($Fe(ClO_4)_3 \cdot 9H_2O$, 98%) from Sigma Aldrich and anhydrous ferric sulfate ($Fe_2(SO_4)_3$, 97%) from Carlo Erba Reagents were Analytical Grade. Hydrogen peroxide (30% by weight not stabilized) was purchased from Fluka.

The pH of BT solutions was regulated with perchloric acid or sulfuric acid-sodium sulfate. $KClO_4$ was used to regulate the ionic strength. Stock solutions were freshly prepared in dark for each run by dissolving the ferric salt in a proper volume of bi-distilled water at an adjusted pH. Solutions were immediately used to avoid the formation, reported by others

[26], of high molecular weight hydrolysis products. No evidence of turbidity or precipitate on 0.25 micron filters was observed, thus ruling out the possibility of formation of colloidal iron oxides.

Each run was carried out by first switching on the lamp without solutions in the reactor and, after the achievement of the maximum irradiating lamp power (10 min), by rapidly feeding the solutions to the reactor.

Due to the difficulties to prevent further oxidation after sampling, samples were taken from the reactor and immediately injected and analyzed. The concentration of the substrate was evaluated by HPLC analysis. For this purpose, the HPLC apparatus was equipped with a UV–VIS detector ($\lambda = 220$ nm) and a Phenomex C6 reverse phase column, using a 80:20 buffered aqueous solution: acetonitrile as mobile phase, flowing at 0.5 ml min^{-1}. The buffered aqueous solution was prepared with 4 ml phosphoric acid, 25 ml methanol in 1 l HPLC water.

All glassware and photolysis tubes were cleaned with hydrochloric acid and washed several times with bi-distilled water before the use. pH measurements were performed by means of an Orion 960 pH-meter.

The power of lamp at 366 nm ($I^0_{(366)}$), recorded using a UV radiometer, was 4.77×10^{-7} einstein s^{-1}, whereas that at 313 nm ($I^0_{(313)}$) was determined with valerophenone actinometry by assuming a quantum yield of 1 mol einstein^{-1} [27]. Valerophenone was analyzed by HPLC, using a water–acetonitrile mixture as the mobile phase. From these measurements a value of 7.97×10^{-7} einstein s^{-1} was obtained.

Hydrogen peroxide was analyzed using an iodometric method. The molar absorptivities (M^{-1} cm^{-1}) for H_2O_2 and BT at $\lambda = 305$, 313 and 366 nm were calculated by measuring the absorbance of a H_2O_2 solution (5.0×10^{-3} M) and BT solution (1.0×10^{-5} M) with UV–VIS spectrophotometer (HP 8452 A) with quartz cells (path length = 1 cm).

A numerical integration program (Matlab) was used to compute the time-concentration profiles.

3. Results and discussion

3.1. Kinetic model

As previously reported photo-assisted Fenton system is characterized by the capability of iron(III) hydroxy complex, $Fe(HO)^{2+}$, to photoreduce:

$$Fe(OH)^{2+} \xrightarrow{h\nu} HO^{\bullet} + Fe^{II}$$

which renders Fe(II) available for the classic Fenton reaction (1).

The system is completely described by means of the following reaction:

$$Fe^{II} + HO^{\bullet} \xrightarrow{k_{Fe^{II}/HO}} Fe^{III} + HO^{-} \quad (3)$$

$$Fe^{II} + HO_2^{\bullet} \xrightarrow{k_{Fe^{II}/HO_2}} Fe(HO_2)^{2+} \quad (4)$$

$$HO_2^{\bullet} \xrightarrow{k_{HO_2^{\bullet}}} H^+ + O_2^{\bullet -} \quad (5)$$

$$H^+ + O_2^{\bullet -} \xrightarrow{k_{O_2^{\bullet -}}} HO_2^{\bullet} \quad (6)$$

$$Fe(HO_2)^{2+} \xrightarrow{k_{Fe(HO_2)^{2+}}} Fe^{II} + HO_2^{\bullet} \quad (7)$$

$$Fe^{III} + HO_2^{\bullet} \xrightarrow{k_{Fe^{III}/HO_2}} Fe^{II} + O_2 + H^+ \quad (8)$$

$$Fe^{III} + H_2O_2 \xrightarrow{k_{Fe^{III}/H_2O_2}} Fe^{II} + HO_2^{\bullet} + H^+ \quad (9)$$

$$Fe^{II} + O_2^{\bullet -} + H^+ \xrightarrow{k_{Fe^{II}/O_2^{\bullet -}}} Fe(HO_2)^{2+} \quad (10)$$

$$Fe^{III} + O_2^{\bullet -} \xrightarrow{k_{Fe^{III}/O_2^{\bullet -}}} Fe^{II} + O_2 \quad (11)$$

$$H_2O_2 \xrightarrow{h\nu} 2HO^{\bullet} \quad (12)$$

$$HO^{\bullet} + H_2O_2 \xrightarrow{k_{HO/H_2O_2}} H_2O_2 + HO_2^{\bullet} \quad (13)$$

$$2HO_2^{\bullet} \xrightarrow{k_t} H_2O_2 + O_2 \quad (14)$$

$$SO_4^{2-} + HO^{\bullet} + H^+ \xrightarrow{k_{HO/HSO_4}} H_2O + SO_4^{\bullet -} \quad (15)$$

$$\text{Substrate} + HO^{\bullet} \xrightarrow{k_c} \text{products} \quad (16)$$

and equilibrium relationships:

$$Fe^{III} + HO^- \overset{K_{Eq.\,(17)}}{\rightleftharpoons} Fe(OH)^{2+} \quad (17)$$

$$Fe(OH)^{2+} + HO^- \overset{K_{Eq.\,(18)}}{\rightleftharpoons} Fe(OH)_2^+ \quad (18)$$

$$Fe(SO_4)^+ \overset{K_{Eq.\,(19)}}{\rightleftharpoons} Fe^{III} + SO_4^{2-} \quad (19)$$

$$SO_4^{2-} + H^+ \overset{K_{Eq.\,(20)}}{\rightleftharpoons} HSO_4^- \quad (20)$$

$$Fe^{III} + H_2O_2 \overset{K_{Eq.\,(21)}}{\rightleftharpoons} Fe(HO_2)^{2+} + H^+ \quad (21)$$

$$Fe(OH)^{2+} + H_2O_2 \overset{K_{Eq.\,(22)}}{\rightleftharpoons} Fe(OH)(HO_2)^+ + H^+ \quad (22)$$

$$FeSO_4 \overset{K_{Eq.\,(23)}}{\rightleftharpoons} Fe^{II} + SO_4^{2-} \quad (23)$$

On the basis of above reported reactions the following mass-balance equations are thus written for all the involved species:

$$\frac{d[Fe^{III}]_T}{dt} = -\frac{F}{V_o} + k_{Fe^{II}/HO}[Fe^{II}][HO^\bullet] + k_{Fe^{II}/H_2O_2}[Fe^{II}][H_2O_2]$$
$$+k_{Fe^{II}/HO_2\bullet}[Fe^{II}][HO_2^\bullet] - k_{Fe(HO_2)^{2+}}[Fe(HO_2)^{2+}]$$
$$-k_{Fe^{III}/HO_2\bullet}[Fe^{III}][HO_2^\bullet] - k_{Fe^{III}/H_2O_2}[Fe^{III}][H_2O_2]$$
$$-k_{Fe^{III}/O_2\bullet^-}[Fe^{III}][O_2^{\bullet-}] + k_{Fe^{II}/O_2\bullet^-}[Fe^{II}][O_2^{\bullet-}] \quad (24)$$

$$\frac{d[Fe^{II}]_T}{dt} = +\frac{F}{V_o} - k_{Fe^{II}/HO}[Fe^{II}][HO^\bullet] - k_{Fe^{II}/H_2O_2}[Fe^{II}][H_2O_2]$$
$$-k_{Fe^{II}/O_2\bullet^-}[Fe^{II}][O_2^{\bullet-}] - k_{Fe^{II}/HO_2\bullet^-}[Fe^{II}][HO_2^\bullet]$$
$$+k_{Fe(HO_2)^{2+}}[Fe(HO_2)^{2+}] + k_{Fe^{III}/HO_2\bullet}[Fe^{III}][HO_2^\bullet]$$
$$+k_{Fe^{III}/H_2O_2}[Fe^{III}][H_2O_2] + k_{Fe^{III}/O_2\bullet^-}[Fe^{III}][O_2^{\bullet-}] \quad (25)$$

$$\frac{d[H_2O_2]}{dt} = -\frac{F_{H_2O_2}}{V_o} - k_{Fe^{II}/H_2O_2}[Fe^{II}][H_2O_2] - k_{HO/H_2O_2}[HO^\bullet][H_2O_2]$$
$$+\frac{k_t}{2}[HO_2^\bullet]^2 - k_{Fe^{III}/H_2O_2}[Fe^{III}][H_2O_2] \quad (26)$$

$$\frac{d[HO_2^\bullet]}{dt} = +k_{HO/H_2O_2}[HO^\bullet][H_2O_2] - k_{Fe^{II}/HO_2\bullet}[Fe^{II}][HO_2^\bullet] - k_t[HO_2^\bullet]^2$$
$$-k_{Fe^{III}/HO_2\bullet}[Fe^{III}][HO_2^\bullet] + k_{Fe(HO_2)^{2+}}[Fe(HO_2)^{2+}]$$
$$+k_{Fe^{III}/H_2O_2}[Fe^{III}][H_2O_2] - k_{HO_2\bullet}[HO_2^\bullet] + k_{O_2\bullet^-}[O_2^{\bullet-}][H^+] \quad (27)$$

$$\frac{d[O_2^{\bullet-}]}{dt} = -k_{Fe^{II}/O_2\bullet^-}[Fe^{II}][O_2^{\bullet-}] - k_{Fe^{III}/O_2\bullet^-}[Fe^{III}][O_2^{\bullet-}]$$
$$+k_{HO_2\bullet}[HO_2^\bullet] - k_{O_2\bullet^-}[O_2^{\bullet-}][H^+] \quad (28)$$

$$\frac{d[HO^\bullet]}{dt} = \frac{1}{V_o}(+F + 2F_{H_2O_2}) - k_{Fe^{II}/HO}[Fe^{II}][HO^\bullet] + k_{Fe^{II}/H_2O_2}[Fe^{II}][H_2O_2] - k_{HO/H_2O_2}[HO^\bullet][H_2O_2] - k_c[S][HO^\bullet] - k_{HO/HSO_4^-}[HO^\bullet][HSO_4^-] \quad (29)$$

$$\frac{d[HSO_4^-]}{dt} = -k_{HO/HSO_4^-}[HO^\bullet][HSO_4^-] \quad (30)$$

where

$$F_{H_2O_2} = \sum_{i=1}^{3}(I^0_{\lambda_i}\Phi^{(H_2O_2)}_{\lambda_i})\left[1 - \exp\left(-2.3L\left(\left(\sum_{i=1}^{3}\varepsilon^{(H_2O_2)}_{\lambda_i}\right)[H_2O_2] + \left(\sum_{i=1}^{3}\varepsilon^{(S)}_{\lambda_i}\right)[S] + \left(\sum_{i=1}^{3}\varepsilon^{(Fe(HO)^{2+})}_{\lambda_i}\right)[Fe(HO)^{2+}] + \left(\sum_{i=1}^{3}\varepsilon^{(Fe(HO_2)^{2+})}_{\lambda_i}\right)[Fe(HO_2)^{2+}] + \left(\sum_{i=1}^{3}\varepsilon^{(Fe(HO)(HO_2)^{2+})}_{\lambda_i}\right)[Fe(OH)(HO_2)^{+}]\right)\right)\right] f_{H_2O_2} \quad (31)$$

$$F = \sum_{i=1}^{3}(I^0_{\lambda_i}\Phi^{(Fe(HO)^{2+})}_{\lambda_i})\left[1 - \exp\left(-2.3L\left(\left(\sum_{i=1}^{3}\varepsilon^{(H_2O_2)}_{\lambda_i}\right)[H_2O_2] + \left(\sum_{i=1}^{3}\varepsilon^{(S)}_{\lambda_i}\right)[S] + \left(\sum_{i=1}^{3}\varepsilon^{(Fe(HO)^{2+})}_{\lambda_i}\right)[Fe(HO)^{2+}] + \left(\sum_{i=1}^{3}\varepsilon^{(Fe(HO_2)^{2+})}_{\lambda_i}\right)[Fe(HO_2)^{2+}] + \left(\sum_{i=1}^{3}\varepsilon^{(Fe(OH)(HO_2)^{2+})}_{\lambda_i}\right)(Fe(OH)(HO_2)^{+})\right)\right)\right] f_{Fe(OH)^{2+}} \quad (32)$$

with $\lambda_1 = 305\,\text{nm}$, $\lambda_2 = 313\,\text{nm}$ and $\lambda_3 = 366\,\text{nm}$ and

$$f_{H_2O_2} = \frac{\left(\sum_{i=1}^{3}\varepsilon_{\lambda_i}^{(H_2O_2)}\right)[H_2O_2]}{\left(\sum_{i=1}^{3}\varepsilon_{\lambda_i}^{(H_2O_2)}\right)[H_2O_2] + \left(\sum_{i=1}^{3}\varepsilon_{\lambda_i}^{(S)}\right)[S] + \left(\sum_{i=1}^{3}\varepsilon_{\lambda_i}^{(Fe(HO))^{2+}}\right)[Fe(HO_2)^{2+}] + \left(\sum_{i=1}^{3}\varepsilon_{\lambda_i}^{(Fe(HO_2))^{2+}}\right)[Fe(HO_2)^{2+}] + \left(\sum_{i=1}^{3}\varepsilon_{\lambda_i}^{(Fe(OH)(HO_2))^{2+}}\right)[Fe(OH)(HO_2)^{2+}]} \tag{33}$$

$$f_{Fe(HO)^{2+}} = \frac{\left(\sum_{i=1}^{3}\varepsilon_{\lambda_i}^{(Fe(HO))^{2+}}\right)[Fe(HO)^{2+}]}{\left(\sum_{i=1}^{3}\varepsilon_{\lambda_i}^{(H_2O_2)}\right)[H_2O_2] + \left(\sum_{i=1}^{3}\varepsilon_{\lambda_i}^{(S)}\right)[S] + \left(\sum_{i=1}^{3}\varepsilon_{\lambda_i}^{(Fe(HO))^{2+}}\right)[Fe(HO)^{2+}] + \left(\sum_{i=1}^{3}\varepsilon_{\lambda_i}^{(Fe(HO_2))^{2+}}\right)[Fe(HO_2)^{2+}] + \left(\sum_{i=1}^{3}\varepsilon_{\lambda_i}^{(Fe(OH)(HO_2))^{+}}\right)[Fe(OH)(HO_2)^{+}]} \tag{34}$$

To calculate the concentration of all iron and sulfate-containing species, four other mass-balance equations need to be added:

$$[Fe^{3+}]_T = [Fe^{3+}] + [Fe(HO)^{2+}] + [Fe(HO)_2{}^{+}] + [Fe(HO_2)^{2+}] + [Fe(OH)(HO_2)^{+}] + [Fe(SO_4)^{+}] \tag{35}$$

$$[Fe^{2+}]_T = [Fe^{2+}] + [FeSO_4] \tag{36}$$

$$[SO_4{}^{2-}]_T = [SO_4{}^{2-}] + [HSO_4{}^{-}] + [FeSO_4] + [Fe(SO_4)^{+}] \tag{37}$$

$$[H_2O_2]_T = [H_2O_2] + [Fe(HO_2)^{2+}] + [Fe(OH)(HO_2)^{+}] \tag{38}$$

along with equilibrium relationships:

$$[Fe(OH)^{2+}] = K_{Eq.(17)}\frac{\gamma_{Fe^{3+}}\gamma_{HO^-}}{\gamma_{Fe(OH)^{2+}}}[Fe^{3+}][HO^-] \tag{39}$$

$$[Fe(OH)_2{}^{+}] = K_{Eq.(17)}K_{Eq.(18)}\frac{\gamma_{Fe^{3+}}\gamma_{HO^-}^2}{\gamma_{Fe(OH)^{2+}}}[Fe^{3+}][HO^-]^2 \tag{40}$$

$$[Fe(HO_2)^{2+}] = K_{Eq.(21)}\frac{\gamma_{Fe^{3+}}}{\gamma_{Fe(HO_2)^{2+}}\gamma_{H^+}}\frac{[Fe^{3+}][H_2O_2]}{[H^+]} \tag{41}$$

Table 1
Rate constants (k_i), equilibrium constants (K_i), quantum yields ($\Phi_{(\lambda_i)}$), UV-light intensities ($I^0_{(\lambda_i)}$) and molar extinction coefficients ($\varepsilon_{(\lambda_i)}$) for kinetic modeling

Parameter	Value	References
k_{HO/H_2O_2}	$3.3 \times 10^7\ M^{-1}\ s^{-1}$	[28]
k_c	$4.64 \times 10^9\ M^{-1}\ s^{-1}$	[19]
k_{HO/HSO_4}	$1.19 \times 10^6\ M^{-1}\ s^{-1}$	[29]
k_t	$8.3 \times 10^5\ M^{-1}\ s^{-1}$	[30]
$k_{Fe^{II}/HO}$	$3.2 \times 10^8\ M^{-1}\ s^{-1}$	[29]
k_{Fe^{II}/H_2O_2}	$63\ M^{-1}\ s^{-1}$	[31]
k_{Fe^{II}/HO_2}	$1.2 \times 10^6\ M^{-1}\ s^{-1}$	[32]
k_{Fe^{III}/HO_2}	$3.3 \times 10^5\ M^{-1}\ s^{-1}$	[34]
$k_{Fe(HO_2)^{2+}}$	$2.7 \times 10^{-3}\ s^{-1}$	[33]
$k_{Fe^{III}/O_2^{-\bullet}}$	$5.0 \times 10^7\ M^{-1}\ s^{-1}$	[35]
$k_{Fe^{II}/O_2^{-\bullet}}$	$1.0 \times 10^7\ M^{-1}\ s^{-1}$	[36]
$k_{HO_2^\bullet}$	$1.58 \times 10^5\ s^{-1}$	[30]
$k_{O_2^{-\bullet}}$	$1.0 \times 10^{10}\ M^{-1}\ s^{-1}$	[30]
k_{Fe^{III}/H_2O_2}	$2.0 \times 10^{-3}\ M^{-1}\ s^{-1}$	[37]
$K_{Eq.\ (17)}$	$6.5 \times 10^{11}\ M^{-1}$	[38]
$K_{Eq.\ (18)}$	$7.08 \times 10^{-5}\ M^{-1}$	[40]
$K_{Eq.\ (19)}$	$3.08 \times 10^{10}\ M$	[39]
$K_{Eq.\ (20)}$	$8.3 \times 10^{-13}\ M^{-1}$	[41]
$K_{Eq.\ (21)}$	3.65×10^{-3}	[42]
$K_{Eq.\ (22)}$	2.0×10^{-4}	[43]
$K_{Eq.\ (23)}$	$5.01 \times 10^{-3}\ M$	[43]
$\Phi^{H_2O_2}_{313}$	3.0×10^{-1} mol einstein^{-1}	[44]
$\Phi^{Fe(HO)^{2+}}_{305}$	0.14 mol einstein^{-1}	[45]
$\Phi^{Fe(HO)^{2+}}_{313}$	0.14 mol einstein^{-1}	[45]
$\Phi^{Fe(HO)^{2+}}_{366}$	0.017 mol einstein^{-1}	[45]
ε^{S}_{305}	$8.2 \times 10\ M^{-1}\ cm^{-1}$	Directly measured
ε^{S}_{313}	$4.0 \times 10\ M^{-1}\ cm^{-1}$	Directly measured
ε^{S}_{366}	$8.0\ M^{-1}\ cm^{-1}$	Directly measured
$\varepsilon^{Fe(HO)^{2+}}_{305}$	$1970\ M^{-1}\ cm^{-1}$	[45]
$\varepsilon^{Fe(HO)^{2+}}_{313}$	$1760\ M^{-1}\ cm^{-1}$	[45]
$\varepsilon^{Fe(HO)^{2+}}_{366}$	$250\ M^{-1}\ cm^{-1}$	[45]
$\varepsilon^{Fe(HO_2)^{2+}}_{305}$	$850\ M^{-1}\ cm^{-1}$	[43]
$\varepsilon^{Fe(HO_2)^{2+}}_{313}$	$600\ M^{-1}\ cm^{-1}$	[43]
$\varepsilon^{Fe(HO_2)^{2+}}_{366}$	$380\ M^{-1}\ cm^{-1}$	[43]
$\varepsilon^{Fe(OH)(HO_2)^{+}}_{305}$	$9900\ M^{-1}\ cm^{-1}$	[43]
$\varepsilon^{Fe(OH)(HO_2)^{+}}_{313}$	$8200\ M^{-1}\ cm^{-1}$	[43]
$\varepsilon^{Fe(OH)(HO_2)^{+}}_{366}$	$1800\ M^{-1}\ cm^{-1}$	[43]
$I^0_{(313)}$	7.97×10^{-7} einstein s^{-1}	Directly measured
$I^0_{(366)}$	4.77×10^{-7} einstein s^{-1}	Directly measured

$$[Fe(OH)(HO_2)^+] = K_{Eq.(21)} K_{Eq.(22)} \frac{\gamma_{Fe^{3+}}}{\gamma_{Fe(HO_2)^{2+}} \gamma_{H^+}^2} \frac{[Fe^{3+}][H_2O_2]^2}{[H^+]^2} \quad (42)$$

$$[Fe(SO_4)^+] = \frac{1}{K_{Eq.(19)}} \frac{\gamma_{Fe^{3+}} \gamma_{SO_4^{2-}}}{\gamma_{Fe(SO_4)^+}} [Fe^{3+}][SO_4{}^{2-}] \quad (43)$$

$$[HSO_4^-] = K_{Eq.(20)} \frac{\gamma_{SO_4^{2-}} \gamma_{H^+}}{\gamma_{HSO_4^-}} [SO_4{}^{2-}][H^+] \quad (44)$$

$$[FeSO_4] = \frac{1}{K_{Eq.(23)}} \gamma_{Fe^{2+}} \gamma_{SO_4^{2-}} [Fe^{2+}][SO_4{}^{2-}] \quad (45)$$

For the estimation of activity coefficients of involved chemical species the Davies' formula was adopted [46]:

$$-\log \gamma = 0.509 z^2 \left[\frac{\sqrt{I}}{1+\sqrt{I}} - 0.2I \right]$$

Table 2
Operating conditions ($T = 293$ K, $[BT]_o = 1.0 \times 10^{-2}$ mM) of experimental runs and statistical analysis[a]

Run (no.)	$[H_2O_2]$ (mM)	[Fe(III)] (mM)	pH	$[ClO_4^-]$ (mM)	$[SO_4{}^{2-}]$ (mM)	I (mM)	σ (%)
1	1.0	1.0×10^{-3}	2.0	30.0	–	59	14.1
2	1.0	2.0×10^{-3}	2.0	30.0	–	59	14.2
3	1.0	4.0×10^{-3}	2.0	30.0	–	59	7.4
4	2.0	2.0×10^{-3}	2.0	30.0	–	59	16.6
5	1.0	1.0×10^{-3}	2.0	–	10	46	4.3
6	1.0	2.0×10^{-3}	2.0	–	10	46	13.5
7	1.0	3.0×10^{-3}	2.0	29.9	2.0×10^{-2}	49	14.0
8	1.0	3.0×10^{-3}	2.7	29.9	2.0×10^{-2}	34	2.0
9	1.0	1.0×10^{-3}	2.7	–	10	34	11.0
10	1.0	2.0×10^{-3}	2.7	–	10	34	9.8
11	1.0	3.0×10^{-3}	2.7	–	10	34	22.0
12	2.0	1.0×10^{-3}	2.7	29.9	2.0×10^{-2}	34	23.1
13	2.0	2.0×10^{-3}	2.7	29.9	2.0×10^{-2}	34	7.0
14	2.0	3.0×10^{-3}	2.7	29.9	2.0×10^{-2}	34	15.0
15	6.0	2.0×10^{-3}	2.7	29.9	2.0×10^{-2}	34	14.4
16	15.0	2.0×10^{-3}	2.7	29.9	2.0×10^{-2}	34	9.0
17	15.0	2.0×10^{-3}	2.7	29.9	2.0×10^{-2}	34	13.0
18	1.0	3.0×10^{-3}	3.2	29.9	2.0×10^{-2}	30	35.9
19	1.0	1.0×10^{-3}	2.0	29.9	2.0×10^{-2}	49	21.5
20	1.0	2.0×10^{-3}	2.7	29.9	2.0×10^{-2}	34	5.4
21	1.0	1.0×10^{-3}	3.0	–	10	30	31.1
22	1.0	1.0×10^{-3}	2.0	10	–	39	14.8
23	1.0	1.0×10^{-3}	2.0	20	–	49	12.1

[a] I: Ionic strength; σ: standard deviation.

By assuming the steady-state hypothesis, the mass-balance Eq. (29) for HO radicals reduces to:

$$[HO]_{ss} = \frac{1/V_o(F + 2F_{H_2O_2}) + k_{Fe^{II}/H_2O_2}[Fe^{II}][H_2O_2]}{k_{Fe^{II}/HO}[Fe^{II}] + k_{HO/H_2O_2}[H_2O_2] + k_c[S] + k_{HO/HSO_4}[HSO_4^-]} \quad (46)$$

and the consumption rate of the substrate can be calculated as

$$\frac{d[S]}{dt} = -k_c[S][HO]_{ss} \quad (47)$$

The use of this model requires that suitable values are available for all the parameters included in the above equations. In Table 1, the values found in the literature or directly measured are shown.

It is clear from this table that no data are available for quantum yields of hydrogen peroxide at 305 and 366 nm. A simple analysis of an absorption spectrum of hydrogen peroxide indicates that at a wavelength of 366 nm the extinction coefficient can be considered as low as negligible with respect to those at 313 nm (2.8×10^{-1} M^1 cm^{-1}) and 305 nm (8.7×10^{-1} M^{-1} cm^{-1}). This consideration allows to simplify the above-written equations in which all the terms due to H_2O_2 absorption at 366 nm can be neglected.

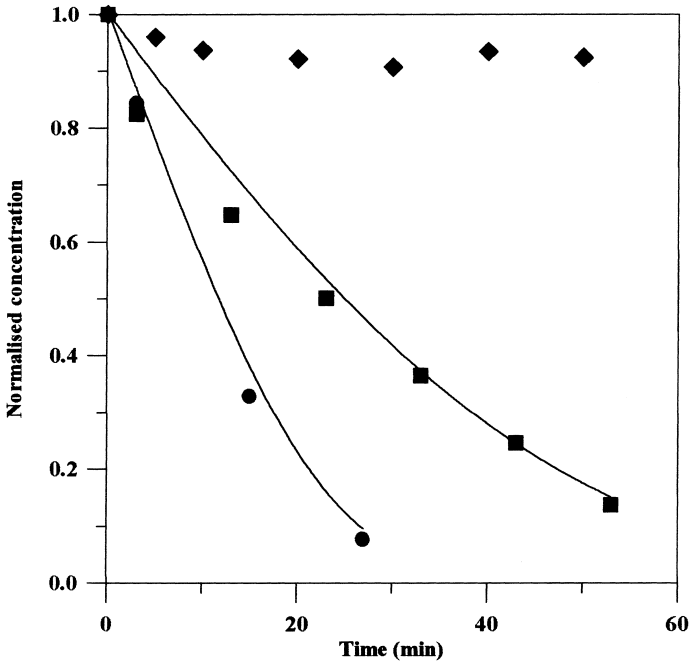

Fig. 1. Effect of sulfate concentration on the system reactivity: predicted (solid lines) and experimental (symbols) concentration-time profile for benzothiazole at pH = 2.7. $[BT]_o = 1.0 \times 10^{-2}$ mM, $[H_2O_2]_T = 1.0$ mM, $[Fe(III)]_T = 2.0\,\mu$M; (●) $[SO_4^{2-}]_T = 2.0 \times 10^{-2}$ mM; (■) $[SO_4^{2-}]_T = 10$ mM; (◆) $[SO_4^{2-}]_T = 10$ mM, without H_2O_2 and Fe(III).

No measured values have been found in the literature for hydrogen peroxide quantum yield at 305 nm. Chang and Young [47] reported that quantum yield for HO radical production is approximately 1.0 mol einstein^{-1} in the range 254–351 nm, whereas Dainton [44] found a quantum yield of 3.0×10^{-1} mol einstein^{-1} at 313 nm. In the present work $\Phi_{254}^{H_2O_2} = 5.0 \times 10^{-1}$, $\Phi_{313}^{H_2O_2} = 3.0 \times 10^{-1}$ mol einstein^{-1} have been adopted and

$$\Phi_{305}^{H_2O_2} \approx \Phi_{313}^{H_2O_2} \tag{48}$$

has been assumed.

Since no direct determination of the irradiating power of lamp at 305 nm was available, photolytic experiments on solutions, at pH 2.70, containing BT (1.0×10^{-5} M), H_2O_2 ($1.0 \times$

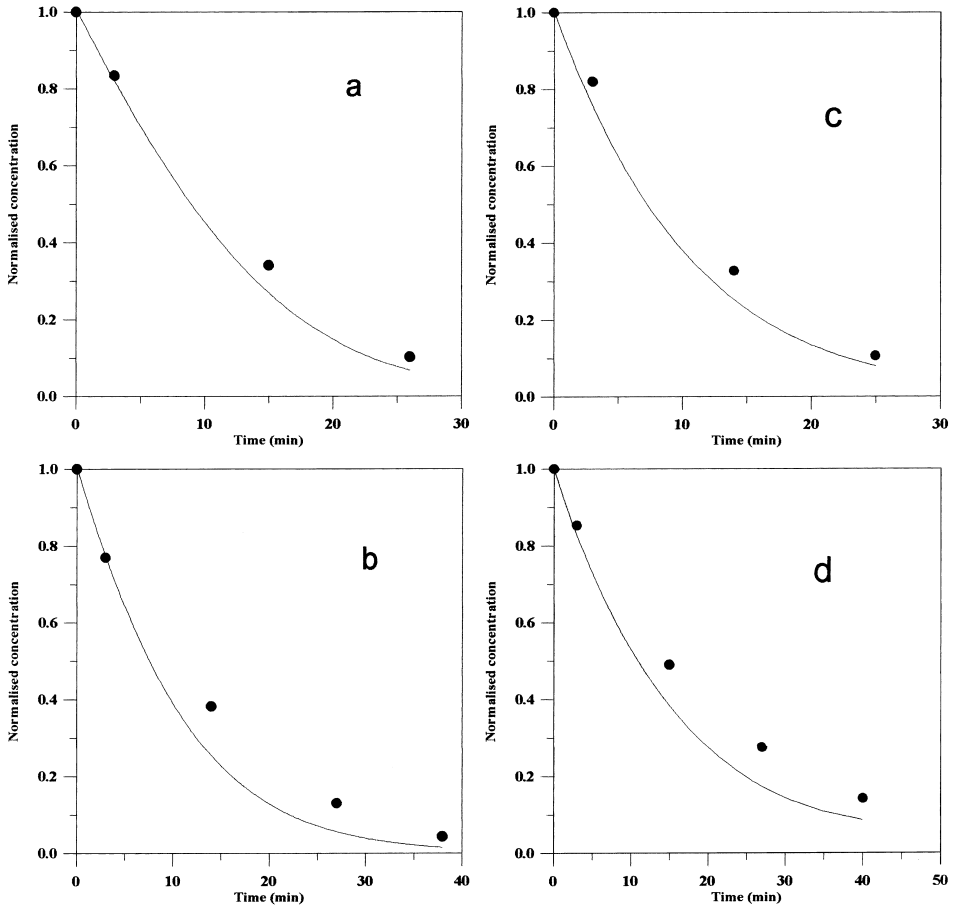

Fig. 2. Effect of hydrogen peroxide concentration on the system reactivity: predicted (solid lines) and experimental (symbols) concentration-time profile for benzothiazole at pH = 2.7. $[BT]_o = 1.0 \times 10^{-2}$ mM, $[SO_4^{2-}]_T = 2.0 \times 10^{-2}$ mM, $[ClO_4^-]_T = 29.9$ mM, $[Fe(III)]_T = 2.0\,\mu$M. (a) $[H_2O_2] = 2.0$ mM; (b) $[H_2O_2] = 6.0$ mM; (c) $[H_2O_2] = 15.0$ mM; (d) $[H_2O_2] = 150.0$ mM.

10^{-2}, 1.5×10^{-2} and 1.5×10^{-1} M), Na_2SO_4 (2.0×10^{-5} M) and $KClO_4$ (29.9×10^{-3} M), with no iron added, were performed.

The analysis of the results of these experiments (considered all as belonging to a single set) with a reduced model [19] based on the reactions (12)–(16) and by using a proper optimization method [48] allowed the estimation of a power lamp at 305 nm equal to $4.33 \times 10^{-7} \pm 2.33 \times 10^{-8}$ einstein s^{-1} ($\sigma\% = 8.0$–10.9).

3.2. Modeling photo-assisted Fenton experiments

The assumption (48) and the estimation of $I^0_{(305)}$ make possible the use of the model to predict the behavior of the system BT/H_2O_2/Fe(III)/UV at varying reaction conditions, all the parameters included in the mass-balance equations being known.

Photolytic experiments on solutions containing BT, H_2O_2 and Fe(III) and irradiated with the UV lamp have been performed aiming at elucidating the effect on the system reactivity of BT, H_2O_2 and Fe(III) concentrations, pH and ionic strength.

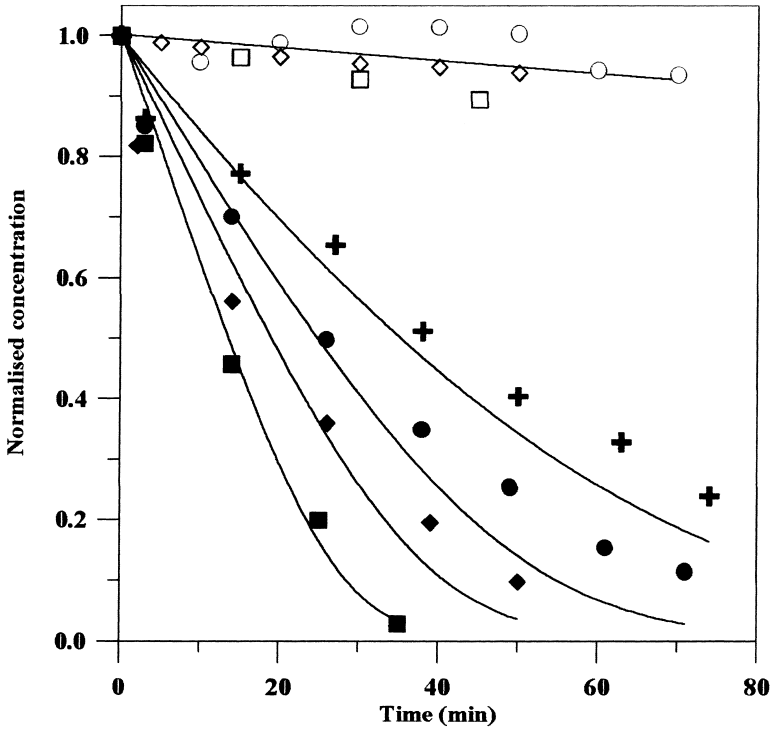

Fig. 3. Effect of iron (III) concentration on the system reactivity: predicted (solid lines) and experimental (symbols) concentration-time profile for benzothiazole (full symbols) and for hydrogen peroxide (empty symbol) at pH = 2.0. $[BT]_o = 1.0 \times 10^{-2}$ mM, $[ClO_4^-]_T = 30.0$ mM, $[H_2O_2]_T = 1.0$ mM. (●, ○) $[Fe(III)]_T = 1.0$ μM; (◆, ◇) $[Fe(III)]_T = 2.0$ μM; (■, □) $[Fe(III)]_T = 4.0$ μM; (+) no Fe(III) added.

In Table 2, the experimental conditions for all the oxidative runs with benzothiazole are reported. The last column of the table shows the percentage standard deviations for benzothiazole (a statistical index of the model adequacy) calculated by using experimental data and those data predicted by the model. All the σ values shown in the table are larger than that found in the analytical determination of benzothiazole (1.16%), thus, indicating the possibility of some model inadequacies. The present kinetic model relies on the implicit assumption (reactions (1)–(16)) that the intermediates formed during the oxidation process have a negligible effect on the rate of consumption of HO radicals. This assumption, done to overcome the difficulties due to the lack of knowledge of the structures and reactivity of these intermediates, could be responsible of these larger percentage standard deviations (σ)

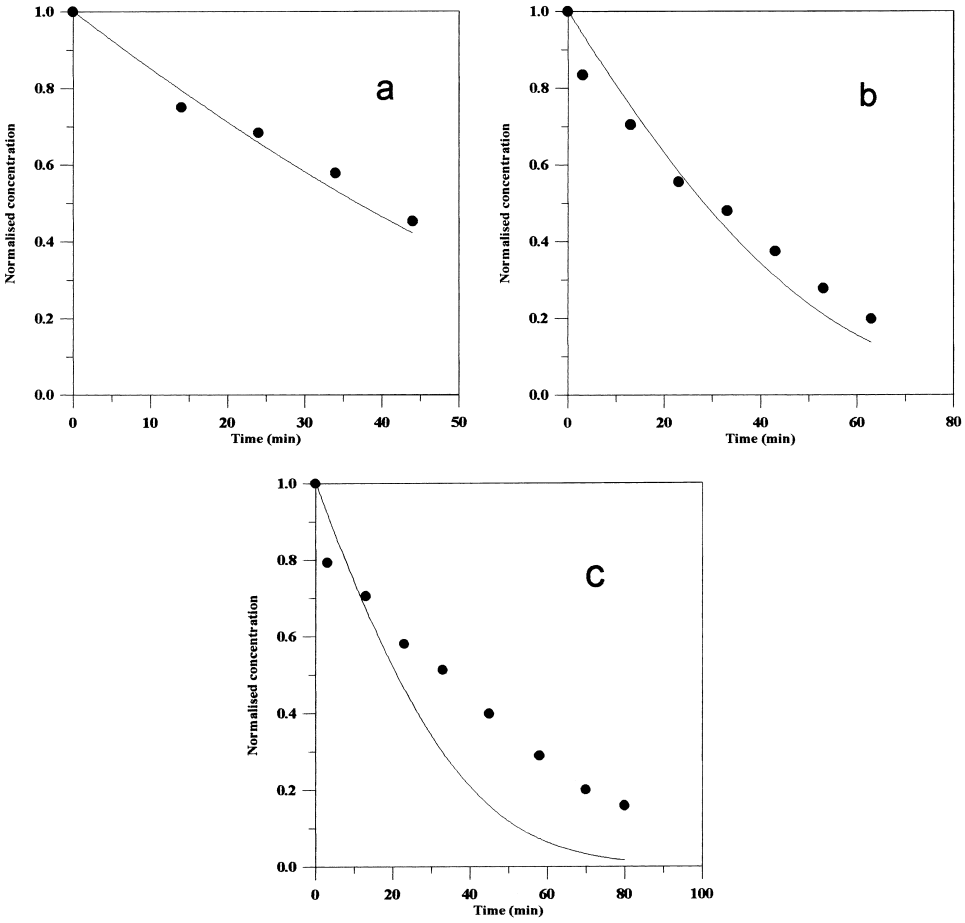

Fig. 4. Effect of pH on the system reactivity. Predicted (solid lines) and experimental (symbols) concentration-time profile for benzothiazole: $[BT]_o = 1.0 \times 10^{-2}$ mM, $[SO_4^{2-}]_T = 10.0$ mM, $[H_2O_2]_T = 1.0$ mM, $[Fe(III)]_T = 1.0$ μM. (a) pH = 2.0; (b) pH = 2.7; (c) pH = 3.0.

at least for the runs at the lowest H_2O_2 concentrations. Runs at fixed hydrogen peroxide and iron (III) concentration and pH indicated that ionic strength has only a small effect on the system reactivity. In fact, at pH = 2.0, for $[H_2O_2] = 1.0 \times 10^{-3}$ M and [Fe(III)] = 1.0×10^{-6} M half-live times are respectively 26 and 23 min for ionic strength equal to 30.0×10^{-3} and 10.0×10^{-3} M, obtained by means of different addition of potassium perchlorate (data not shown).

In Fig. 1, the results of two different runs, with sulfate concentration equal to 10×10^{-3} and 2.0×10^{-5} M (runs nos. 10 and 20 in Table 2), with the same ionic strength adjusted by adding $KClO_4$ salt, are reported. Satisfactory agreement is observed between calculated and experimental data.

In Figs. 2 and 3a comparison of the experimental data and those calculated by the model at varying, respectively, hydrogen peroxide (runs nos. 13, 15–17 in Table 2) and Fe^{III} (runs nos. 1–3) concentrations is reported. In both cases the accuracy of the prediction changes for some runs (see percentage standard deviations in Table 2), although no indications have been found to explain this behavior.

In Fig. 4a comparison of experimental and calculated decay of benzothiazole concentration is reported at varying pH of the solution (runs nos. 5, 9 and 21). Satisfactory results are obtained at pH = 2.0 and 2.7 whereas a complete failure of the model is observed at pH equal 3.0. At pH = 3.2 (run no. 18), σ as large as 35.9 is calculated thus suggesting that the system behavior could be regulated by other reactions, not included in the model. Some authors [45] report at these pH values the formation of Fe(III)-hydroxy complex, such as $[Fe_2(OH)_2]^{4+}$, which photolyzes too. However, in these conditions iron speciation may be hardly calculated — and the kinetics quantitatively interpreted — due to the slow precipitation of iron (III) oxides-which delay the establishment of an equilibrium condition between the solution and the solid phase [49].

4. Conclusion

A kinetic model has been developed to simulate the oxidation in aqueous solution of benzothiazole with the photo-assisted Fenton system in a batch reactor. The model has been tested with the data collected during oxidation experiments of benzothiazole in the pH range 2.0–3.2 at varying hydrogen peroxide and iron(III) concentrations. The model gave satisfactory results when used to predict the influence of H_2O_2, iron(III) and sulfate concentration on the system reactivity. Poor results have been on the other hand partly obtained at varying pH of the solution.

List of symbols

I	ionic strength
I^0	light intensity
k	kinetic constant
K	equilibrium constant
L	reactor optical length
V_o	irradiated reactor volume
z	valency

Greek letters

ε	molar extinction coefficients
γ	activity coefficient
λ	wavelenght
σ	standard deviation
Φ	quantum yield

Subscripts

c	substrate (benzothiazole)
ss	steady state
t	termination
Fe^{2+}	uncomplexed ferryl ion
Fe^{3+}	uncomplexed ferric ion
$HO_2^{\bullet}$	hydroperoxyl radical
$HO^{\bullet}$	hydroxyl radical
$O_2^{\bullet -}$	superoxyl radical

Superscripts

S	substrate
$Fe(OH)^{2+}$	Fe^{III}-hydroxy complex
$Fe(OH_2)^{+}$	Fe^{III}-hydroxy complex
$Fe(OH)(OH_2)^{+}$	Fe^{III}-hydroxy complex
H_2O_2	hydrogen peroxide

Acknowledgements

The authors are very grateful to A. Bizzarro for technical support in the experimental runs and analytical methods.

References

[1] M.C. Lu, J.N. Chen, C. P Chang, Oxidation of dichlorvos with hydrogen peroxide using ferrous ion as catalyst, J. Haz. Mat. B 65 (1999) 277–288.
[2] C.T. Chen, A.N. Tafuri, M. Rahman, M.B. Forest, Chemical oxidation treatment of petroleum contaminated soil using Fenton's reagent, J. Environ. Sci. Health A 33 (1998) 987–1008.
[3] E.G. Solozhenko, N.M. Soboleva, V.V. Goncharuk, Decolourization of azodye solutions by Fenton's oxidation, Water Res. 29 (9) (1995) 2206–2210.
[4] C.M. Miller, R.L. Valentine, Role of superoxide anion in contaminant degradation by hydrogen peroxide in the presence of sandy aquifer material, 212th ACS National Meeting, Book of Abstracts, Orlando, FL, 25–29 August 1996.
[5] R.J. Watts, M.D. Udell, S. Kong, S.W. Leung, Fenton-like soil remediation catalyzed by naturally occurring iron minerals, Environ. Eng. Sci. 16 (1) (1999) 93–97.
[6] R.J. Watts, A.P. Jones, Chen Ping-Hung, A. Kenny, Mineral-catalyzed Fenton-like oxidation of sorbed chlorobenzenes, Water Environ. Res. 69 (3) (1997) 269–275.
[7] J.J. Pignatello, Dark, Environ. Sci. Technol. 26 (1992) 944–951.

[8] J.J. Pignatello, L.Q. Huang, Degradation of polychlorinated dibenzo-p-dioxin and dibenzofuran contaminants in 2,4,5-T by photoassisted iron-catalyzed hydrogen peroxide, Water Res. 27 (12) (1993) 1731–1736.
[9] J. Kiwi, C. Pulgarin, P. Peringer, M. Gratzel, Beneficial effect of homogeneous photo-Fenton pretreatment upon the biodegradation of anthraquinone silfonate in wastewater treatment, Appl. Catal. B: Environ. 3 (1993) 85.
[10] J.J. Pignatello, Y. Sun, Complete oxidation of metolachlor and methylparathion in water by the photoassisted Fenton reaction, Water Res. 57 (8) (1995) 1837–1844.
[11] Safarzadeh-Amiri, J.R. Bolton, S.R. Cater, The use of iron in advanced oxidation processes, J. Adv. Oxid. Technol. 1 (1) (1996) 18–26.
[12] N. Brand, G. Mailhot, M. Bolte, Degradation photoinduced by Fe(III): method of alkylphenol ethoxylates removal in water, Environ. Sci. Technol. 32 (1998) 2715–2720.
[13] S.M. Kim, A. Vogelpohl, Degradation of organic pollutants by the photo-Fenton process, Chem. Eng. Technol. 21 (2) (1998) 187–190.
[14] M.A. Engwall, J.J. Pignatello, D. Grasso, Degradation and detoxification of the wood preservatives creosote and pentachlorophenol in water by the photo-Fenton reaction, Water Res. 33 (5) (1999) 1151–1158.
[15] F. Herrera, J. Kiwi, A. Lopez, V. Nadtochenko, Photochemical decoloration of Remazol Brillant Blue and Uniblue A in the presence of Fe^{3+} and H_2O_2, Environ. Sci. Technol. 33 (1999) 3145–3151.
[16] P.L. Huston, J.J. Pignatello, Degradation of selected pesticide active ingredients and commercial formulations in water by the photo-assisted Fenton reaction, Water Res. 33 (5) (1999) 1238–1246.
[17] J.J. Pignatello, D. Liu, P. Huston, Evidence for an additional oxidant in the photoassisted Fenton reaction, Environ. Sci. Technol. 33 (11) (1999) 1832–1839.
[18] J.M. Herrmann, Heterogeneous photocatalysis: fundamentals and applications to the removal of various types of aqueous pollutants, Catal. Today 53 (1) (1999) 115–129.
[19] R. Andreozzi, V. Caprio, R. Marotta, Oxidation of benzothiazole, 2-mercaptobenzothiazole and 2-hydroxybenzothiazole in aqueous solution by means of H_2O_2/UV or photoassisted Fenton, Water Res. (2000) submitted for publication.
[20] G.A. Jungclaus, L.A. Games, R.A. Hites, Identification of trace organic compounds in tire manufacturing plant wastewaters, Anal. Chem. 48 (13) (1976) 1894–1896.
[21] B.G. Brownlee, J.H. Carey, G.A. McInnis, I.T. Pellizzari, Aquatic environmental chemistry of 2-(thiocyanomethylthio)benzothiazole and related benzothiazoles, Environ. Toxicol. Chem. 11 (1992) 1153–1168.
[22] T. Reemtsma, M. Jekel, Dissolved organics in tannery wastewaters and their alteration by a combined anaerobic and aerobic treatment, Water Res. 31 (5) (1997) 1035–1046.
[23] J. Chudoba, F. Tucek, K. Zies, Biochemischer Abbau von Benzothiazolderivaten, Acta Hydrochim. Hydrobiol. 5 (1977) 499–501.
[24] T. Reemtsma, O. Fiehn, G. Kalnowski, M. Jekel, Microbial transformation and biological effects of fungicide-derived benzothiazoles determined in industrial wastewater, Environ. Sci. Tech. 29 (1995) 478–485.
[25] H. De Wever, H. Verachtert, Biodegradation and toxicity of benzothiazoles, Water Res. 31 (11) (1997) 2673–2684.
[26] R.J. Knight, R.N. Sylva, Spectrophotometric investigation of iron(III) hydrolysis in light and heavy water at 25°C, J. Inorg. Nucl. Chem. 37 (1975) 779–783.
[27] R. Zepp, 1989. US Environmental Protection Agency, College Station road, Athens, personal communication.
[28] H. Christensen, K. Sehested, H. Corfitzen, Reactions of hydroxyl radicals with hydrogen peroxide at ambient and elevated temperatures, J. Phys. Chem. 86 (1982) 1588–1590.
[29] G.V. Buxton, C.L. Greenstock, W.P. Helman, A.B. Ross, Critical review of rate constants for reactions of hydrated electrons, hydrogen atoms and hydroxyl radicals (OH/O^-) in aqueous solution, J. Phys. Chem. Ref. Data 17 (2) (1988) 513–886.
[30] B.H.J. Bielski, D.E. Cabelli, R.L. Arudi, A.B. Ross, Reactivity of HO_2/O_2^- radicals in aqueous solution, J. Phys. Chem. Ref. Data 14 (4) (1985) 1041–1100.
[31] H. Gallard, J. De Laat, B. Legube, Influence du pH sur la vitesse d'oxydation de composès organiques par Fe^{II}/H_2O_2. Mécanismes reactionnels et modélisation, New J. Chem. (1998) 263–268.
[32] G.G. Jayson, B.J. Parson, A.J. Swallow, Oxidation of ferrous ions by perhydroxyl radicals, J. Chem. Soc., Faraday Trans. I 69 (1973) 236–242.

[33] J. De Laat, H. Gallard, Catalytic decomposition of hydrogen peroxide by Fe(III) in homogeneous aqueous solution: mechanism and kinetic modeling, Environ. Sci. Technol. 33 (1999) 2726–2732.
[34] F. Haber, J. Weiss, The catalytic decomposition of hydrogen peroxide by iron salts, Proc. R. Soc. Ser. T27 (1934) 332–351.
[35] W.G. Rothschild, A.O. Allen, Studies in the radiolysis of ferrous sulfate solutions. III. Air free solutions at higher pH, Radiation Res. 8 (1958) 101–110.
[36] J.D. Rush, B.H. Bielski, Pulse radiolytic studies of the reactions of HO_2/O_2^- with Fe(II)/Fe(III) ions. The reactivity of HO_2/O_2^- with ferric ions and its implication of the occurrence of the Haber–Weiss reaction, J. Phys. Chem. 89 (23) (1985) 5062–5066.
[37] S. Lin, M.D. Gurol, Catalytic decomposition of hydrogen peroxide on iron oxide: kinetics, mechanism and implications, Environ. Sci. Technol. 32 (1998) 1417–1423.
[38] J. Weschler, M.L. Mandlich, T.E. Graedel, Speciation, photosensitivity and reactions of transition metal ions in atmospheric droplets, J. Geophys. Res. 91 (1986) 5189–5204.
[39] T.E. Graedel, M.L. Mandlich, C.J. Weschler, Kinetic model studies of atmospheric droplet chemistry. 2. Homogeneous transition metal chemistry in raindrops, J. Geophys. Res. 91 (1986) 5205–5221.
[40] L.G. Sillén, Stability constants of metal-ion complexes. Section I: inorganic ligands, Special publication No. 17, The Chemical Society, Burlington House, W.1 London, 1964, p. 240.
[41] R.C. Weast, 1968. Handbook of Chemistry and Physics, 49th Edition, Chemical Rubber Co., Cleveland, OH, 44128, p. D91.
[42] C. Walling, A. Goosen, Mechanism of the ferric ion catalyzed decomposition of hydrogen peroxide. Effect of organic substrates, J. Am. Chem. Soc. 95 (9) (1973) 2987–2991.
[43] H. Gallard, J. De Laat, B. Legube, Spectrophotometric study of the formation of iron(III)-hydroperoxy complexes in homogeneous aqueous solutions, Water Res. 33 (13) (1999) 2929–2936.
[44] F.S. Dainton, The primary quantun yield in the photolysis of hydrogen peroxide at 313 nm and the primary radical yield in the X- and γ-radiolysis of water, J. Am. Chem. Soc. 78 (1956) 1278–1279.
[45] B.C. Faust, J. Hoigné, Photolysis of Fe(III)-hydroxy complexes as sources of OH radicals in clouds, fog and rain, Atm. Environ. 24 (1) (1990) 79–89.
[46] J.N. Butler, Ionic Equilibrium, Addison-Wesley, New York, 1964.
[47] P.B.L. Chang, T.M. Young, Kinetic of methyl *tert*-butyl ether degradation and by-product formation during UV/hydrogen peroxide water treatment, Water Res. 34 (8) (2000) 2233–2240.
[48] G.V. Reklaitis, A. Ravindran, K.M. Regsdell, Engineering Optimization, Wiley, New York, 1983.
[49] M.E. Balmer, B. Sulzberger, Atrazine degradation in irradiated iron/oxalate systems: effects of pH and oxalate, Environ. Sci. Technol. 33 (1999) 2418–2424.